

Article

# Trapping Analysis of AlGa<sub>N</sub>/Ga<sub>N</sub> Schottky Diodes via Current Transient Spectroscopy

Martin Florovič, Jaroslava Škriniarová, Jaroslav Kováč \* and Peter Kordoš

Institute of Electronics and Photonics, Slovak University of Technology, SK-81219 Bratislava, Slovakia; martin.florovic@stuba.sk (M.F.); jaroslava.skriniarova@stuba.sk (J.Š.); peter.kordos@savba.sk (P.K.)

\* Correspondence: jaroslav.kovac@stuba.sk; Tel.: +421-2-602-91-652

Academic Editor: Farid Medjdoub

Received: 18 March 2016; Accepted: 5 May 2016; Published: 10 May 2016

**Abstract:** Trapping effects on two AlGa<sub>N</sub>/Ga<sub>N</sub> Schottky diodes with a different composition of the AlGa<sub>N</sub> barrier layer were analyzed by current transient spectroscopy. The current transients were measured at a constant bias and at six different temperatures between 25 and 150 °C. Obtained data were fitted by only three superimposed exponentials, and good agreement between the experimental and fitted data was achieved. The activation energy of dominant traps in the investigated structures was found to be within 0.77–0.83 eV. This nearly identical activation energy was obtained from current transients measured at a reverse bias of −6 V as well as at a forward bias of +1 V. It indicates that the dominant traps might be attributed to defects mainly associated with dislocations connected predominantly with the Ga<sub>N</sub> buffer near the AlGa<sub>N</sub>/Ga<sub>N</sub> interface.

**Keywords:** AlGa<sub>N</sub>/Ga<sub>N</sub>; Schottky diode; exponential function; (de)trapping; activation energy

## 1. Introduction

The Ga<sub>N</sub>-based heterostructure field-effect transistors (HFETs) are promising devices for high-frequency and high-power applications. Although such devices are commercially produced, their reliability problems caused by trap-related effects are still under investigation [1,2]. The existence of defects can result from surface states, point defects, and threading dislocations in the AlGa<sub>N</sub>/Ga<sub>N</sub> material structure. Such defects lead to a high leakage current [3], kink effects [4], a current collapse [5], or capacitance hysteresis [6]. They can all significantly influence the performance and reliability of the devices. Therefore, the trap-related processes are systematically studied.

Various methods are used to investigate trapping effects in semiconductors, especially in Ga<sub>N</sub>-based devices. The most popular one is deep-level transient spectroscopy (DLTS), which can be performed in capacitance-mode (C-DLTS) [7–9] or current-mode (I-DLTS) [10–12]. However, capacitance or current transient measurement on real HFET devices can be limited to a degree because of their small dimensions. Resulting inaccuracy might be one of the reasons for a large number of energy levels being reported on Ga<sub>N</sub>-based devices using DLTS methods (see Table I in Ref. [2]). To circumvent the limitation, experiments on large-area Schottky diodes (SDs) can be performed [13,14], provided different electric field distribution between HFETs and SDs are considered. Other commonly used methods are based on the measurement of frequency-dependent conductance [15], low-frequency noise [16], transconductance non-linearity [17], and capacitance–voltage characterization concerning hysteresis [18]. As an extension of the current-mode DLTS, current-transient analysis utilizing a multiexponential decay fitting was also proposed [19]. However, such a procedure has not been generally used at present due to the necessity of using a more complicated fitting technique. These studies are aimed at the identification of trap states energies and their origin. Trap states with energies between 0.43 and 0.50 eV (e.g., [14,17,20,21]) and between 0.71 and 0.82 eV (e.g., [1,9,19,22–24]) were the most commonly reported. Unfortunately, their origin remains ambiguous. As to the traps with the

lower energy range, it is supposed that their source is related to the AlGaN barrier below the gate, surface states, and oxygen related defects in the bulk. However, the origin of those within the higher energy range is attributed to carbon, Fe, or surface-related defects as well as dislocations connected predominantly with the GaN buffer near the AlGaN/GaN interface. Some papers report only trap state energies, leaving their source unspecified.

This study reports on an analysis of trapping effects in two different AlGaN/GaN SD structures. They differ in the AlGaN barrier composition. The current transients at a constant bias were measured in a broad range at different temperatures. Data obtained were fitted by three superimposed exponentials, assuming that the trapping effects had an exponential decay with time. From the temperature-dependent time constants, corresponding to the larger amplitudes, an Arrhenius plot was constructed, and the activation energy of the dominant trap states was evaluated. Both samples exhibited nearly the same activation energy of 0.77–0.83 eV for forward and reverse bias. One can conclude that the associated trap states might be related to defects near the AlGaN/GaN interface.

## 2. Experimental

Two types of AlGaN/GaN heterostructure were used in this work. Both were grown by a metalorganic chemical vapor deposition technique on a 4H-SiC substrate. They differed in the composition of the AlGaN barrier layer. The structures consisted of an AlN nucleation layer, followed by a 1.7- $\mu\text{m}$  GaN buffer layer doped by Fe away from the channel. Figure 1 shows that an AlGaN layer with an AlN mole fraction of 0.25 (Sample A) and 0.29 (Sample B) was grown on top of the buffer. Sample B contained a 1.25-nm AlN interlayer between GaN and AlGaN. The devices were prepared with conventional processing steps, which are typically used in the technology of GaN-based devices. Ohmic contacts were prepared by thermal evaporation of a multilayered Nb/Ti/Al/Ni/Au metal stack and subsequent rapid thermal annealing at 850 °C for 35 s in a  $\text{N}_2$  atmosphere. Mesa isolation was then formed by reactive ion etching in a  $\text{CCl}_4/\text{He}$  plasma. Ni/Au gate electrodes were finally deposited and formed by a lift-off process. SDs with a contact area of  $100 \times 100$  and  $200 \times 200 \mu\text{m}^2$  were prepared and used in our experiments. The current-voltage ( $I$ - $V$ ) characteristics and the current transients in a time range of  $\sim 10^{-3}$  to  $\sim 10^4$  s were measured using a semiconductor parameter analyzer Agilent 4155C and a microprobe station. Measurement was performed in a temperature range between 25 and 150 °C using a heated plate and an ATT Systems A150 temperature controller.

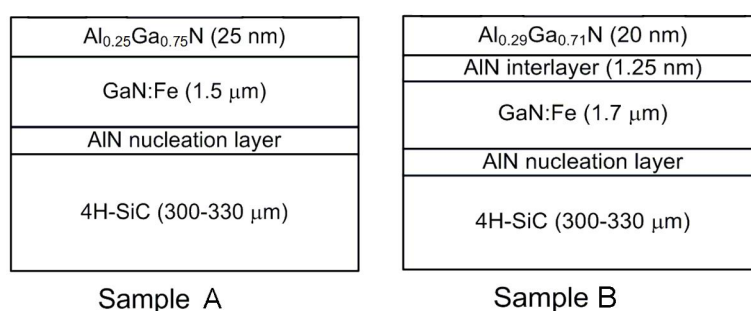
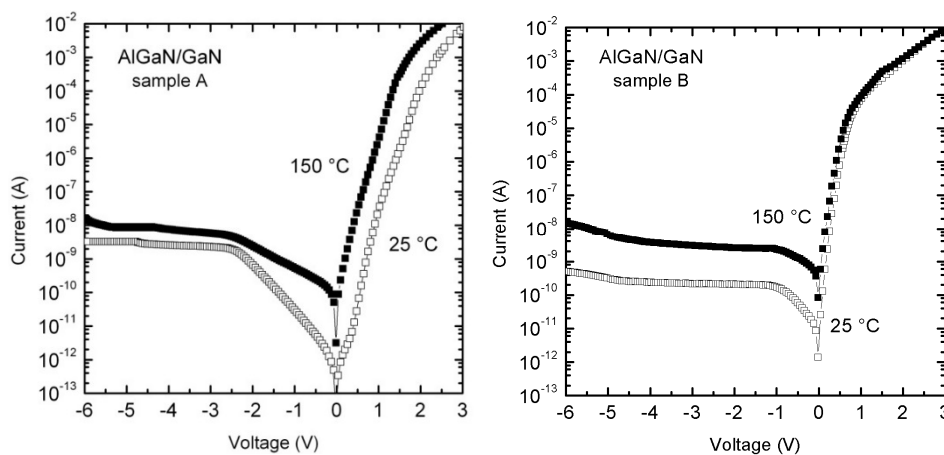


Figure 1. Schematic cross section description of used AlGaN/GaN heterostructures.

## 3. Results and Discussion

Figure 2 shows typical  $I$ - $V$  characteristics for SD Samples A and B measured at the lowest and highest temperature. Due to different AlGaN compositions, one example of which being a thin AlN interlayer, there is a considerable increase in serial resistance in forward  $I$ - $V$  characteristics over 1 V, as visible for Sample B. In addition, the Schottky barrier height at room temperature was evaluated from the forward bias data using a procedure we have previously described [25]. Values of 1.25 eV (Sample A) and 1.34 eV (Sample B) were obtained. The Schottky barrier height influences the high temperature  $I$ - $V$  characteristics behavior by increasing the thermionic emission current. This effect is more visible

for Sample A at 150 °C. Similarly, the reverse current at  $-6$  V was found to be  $3.3 \times 10^{-9}$  A (Sample A) and  $5 \times 10^{-10}$  A (Sample B), which corresponds to the influence of the AlN interlayer in Sample B. A capacitance-voltage measurement was used to evaluate the sheet charge density in the channel, according to the equation  $n_s = \int C \cdot dV$ . The measurement at 100 kHz yielded values of  $1 \times 10^{13} \text{ cm}^{-2}$  and  $7 \times 10^{12} \text{ cm}^{-2}$  for Samples A and B, respectively. The difference in AlGaIn layer thickness and sheet charge density shifts the threshold voltage of the HFET structure, which is clearly visible in reverse  $I$ - $V$  characteristic saturation at  $\sim -2.2$  V and  $\sim -1$  V for Samples A and B, respectively.



**Figure 2.** Typical  $I$ - $V$  characteristics for SD structures A and B measured at 25 °C and 150 °C.

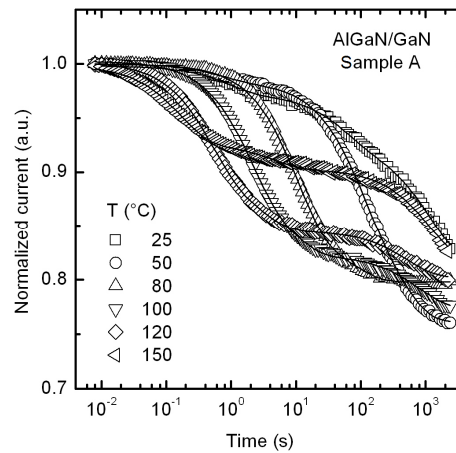
Time-dependent current transients were measured at a constant bias and temperature to evaluate trapping effects in the structures. After measurements, the sample illumination is needed to recover the device states. This was performed by commercial white LED (5000 mcd at 20 mA) illumination for one minute at a zero applied voltage after each transient measurement run. The time-dependent current transients were fitted by exponential functions, *i.e.*, according to the following equation:

$$I_{fitted} = \sum_{i=1}^n A_i \exp(-t/\tau_i) + I_{\infty},$$

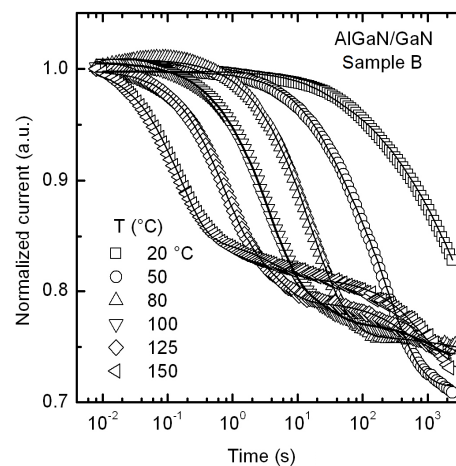
where  $A_i$  is the amplitude, and  $\tau_i$  is the time constant which needs to be evaluated. It was assumed that the trapping effect had an exponential decay with time. An  $A_i = f(\tau_i)$  diagram is usually constructed to show one or more peaks, indicating a trapping effect at a given time constant  $\tau_{peak}$ . An Arrhenius plot ( $\tau_{peak} \cdot T^2$ ) vs.  $1/kT$  is finally constructed from the current transients measured at different temperatures. This allows for the evaluation of the activation energy of dominant trap states. However, usually a large number of exponentials needs to be used to construct an  $A_i = f(\tau_i)$  diagram, e.g., Joh and del Alamo used 100 exponentials [19], and Hu *et al.* as many as 400 [14]. As is shown below, we were able to fit our data satisfactorily with only three exponentials. A similar simple procedure was also used in Bisi *et al.* [2]. The activation energy of a dominant trap was obtained simply from evaluated  $\tau_{peak}$  data for maximal  $A_i$  values at different temperatures. This procedure makes the evaluation of such an experiment much simpler and faster without compromising accuracy.

The SD current transients were measured in a time range between  $\sim 10^{-3}$  s and  $\sim 10^4$  s and at six values of temperature between 25 °C and 150 °C. Two different voltages—a reverse bias of  $-6$  V, and a forward bias of 1 V—were used. A typical result of the current transients measured at  $-6$  V at different temperatures for both samples used in this study is shown in Figures 3 and 4. A decrease of the current with time was observed for both samples. The effect became more significant at an increased temperature. At room temperature, the current decreased to about 83% of its initial value for both samples at the end of the experiment (after  $\sim 40$  min). An overall look at the data, mainly measured

at higher temperatures, indicates that the curves consist of two to three superimposed exponentials. Therefore, the measured current transients were fitted by a sum of only three exponentials, according to the aforementioned equation. The resulting fitted curves are shown in Figures 3 and 4 as full lines. Good agreement between the measured data and fitted curves was obtained for both samples. Similar current transients at various temperatures were measured on both samples at a forward bias of 1 V.

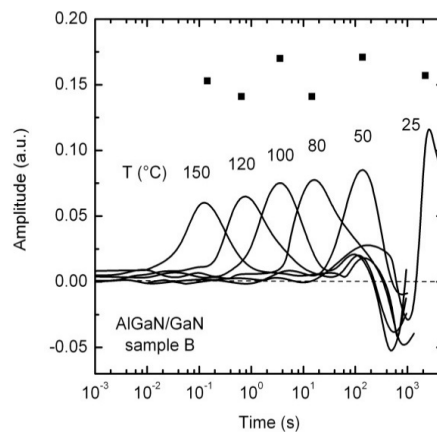


**Figure 3.** Current transients of the AlGaN/GaN structure of Sample A measured at a reverse bias of  $-6$  V at various temperatures. Full lines are fitting curves.



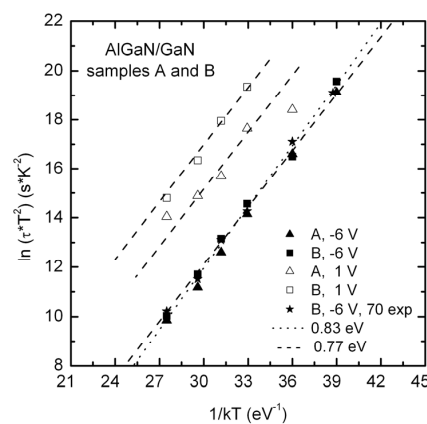
**Figure 4.** Current transients of the AlGaN/GaN structure. Sample B measured at a reverse bias of  $-6$  V at various temperatures. Full lines are fitting curves.

Figure 5 shows for comparison the result of current transients fitting for AlGaN/GaN Sample B using 70 exponentials. Unambiguous temperature-dependent peaks, which shifted to a shorter time with increased temperature, were identified. Other peaks with negative amplitude are nearly temperature-independent, *i.e.*, they cannot be used for the activation energy evaluation. Results obtained from a simple fitting by a “three-exponential” procedure are also shown in Figure 5 (full square marks). Nearly identical  $\tau_{\text{peak}}$  data for maximal  $A_i$  values at different temperatures were obtained.



**Figure 5.** Time constant spectrum of an AlGaIn/GaN SD structure (Sample B,  $V = -6$  V) evaluated by a fitting of the current transients by 70 exponentials. For comparison, data of  $A_i$  vs.  $\tau_i$  obtained from simple three-exponential fitting (full square marks) are also shown.

The  $\tau_i$  data obtained for maximal  $A_i$  values at different temperatures were used to draw a  $(\tau_{\text{peak}} \cdot T^2)$  vs.  $1/kT$  plot for both SD Samples A and B, and the activation energy of dominant trap states was evaluated. Other  $\tau_i$  data show very low corresponding  $A_i$  values, or they did not change significantly with temperature (they were not useful for the evaluation of the activation energy). Figure 6 shows a summary of the obtained  $\tau_{\text{peak}}$  data at different temperatures, *i.e.*, an  $(\tau_{\text{peak}} \cdot T^2)$  vs.  $1/kT$  dependence. The activation energy 0.77–0.83 eV as the dominant trap state can be evaluated for investigated samples. It is of note that the activation energy for the SDs in Sample A, *i.e.*, with a lower AlN content in the barrier, was evaluated in the lower part of the energy range 0.77–0.83 eV mentioned above and for the SDs in Sample B the energy was in the upper part. However, there was only a slight difference ( $\Delta x \cong 0.04$ ) in the barrier composition of the samples investigated. This indicates that nearly identical trap states are present in both SD Samples A and B. In comparison with published data, the traps with activation energies in the 0.6–0.8 eV range are usually found to be located in the GaN buffer near the AlGaIn/GaN interface [24], and, in the 0.8–0.85 eV range, the dominant traps might be attributed to defects mainly associated with dislocations as commonly observed in MOCVD-grown of undoped and Fe-doped GaN layers [1]. From these results, one can assume that the trap states in the investigated SDs are connected predominantly with the GaN buffer near the AlGaIn/GaN interface defects associated with dislocations.



**Figure 6.** Arrhenius plot of the time constant for AlGaIn/GaN SDs (Samples A and B) measured at reverse bias  $-6$  V (full marks) and forward bias  $+1$  V (open marks). For comparison, data obtained by fitting with 80 exponentials are also shown (full stars). Dashed lines correspond to the energy of 0.77 and 0.83 eV.

#### 4. Conclusions

In conclusion, trapping effects on AlGa<sub>N</sub>/Ga<sub>N</sub> Schottky barrier diodes were studied by current transient analysis at different temperatures. Obtained data were fitted by three superimposed exponentials. Nearly the same activation energy of observed traps 0.77–0.83 eV was found in two samples with a slightly different AlGa<sub>N</sub> barrier composition. This energy range follows from measurements at forward (+1 V) and reverse (−6 V) bias voltages. This indicates that the observed trap states might be assigned to the Ga<sub>N</sub> buffer near the AlGa<sub>N</sub>/Ga<sub>N</sub> interface defects associated with dislocations.

**Acknowledgments:** This work was supported by the Slovak Grant Agency VEGA (Grant Nos. 1/0491/15 and 1/0739/16). The authors would like to thank A. Chvála for the Schottky barrier evaluation.

**Author Contributions:** All authors participated equally in the creation of the text and in the presentation and discussion of the results.

**Conflicts of Interest:** The authors declare that there is no conflict of interest.

#### References

1. Polyakov, J.A.Y.; Lee, I.H. Deep traps in Ga<sub>N</sub>-based structures as affecting the performance of Ga<sub>N</sub> devices. *Mater. Sci. Engn.* **2015**, *94*, 1–56.
2. Bisi, D.; Meneghini, M.; de Santi, C.; Chini, A.; Dammann, M.; Brückner, P.; Mikulla, M.; Meneghesso, G.; Zanoni, E. Deep-level characterization in Ga<sub>N</sub> HEMTs-Part I: Advantages and limitations of drain current transient measurements. *IEEE Trans. Electron Devices* **2013**, *60*, 3166–3175. [[CrossRef](#)]
3. Saadaoui, S.; Salem, M.M.B.; Fathallah, O.; Gassoumi, M.; Gaquière, C.; Maaref, H. Leakage current, capacitance hysteresis and deep traps in Al<sub>0.25</sub>Ga<sub>0.75</sub>N/GaN/SiC high-electron-mobility transistors. *Phys. B: Condens. Matter* **2013**, *412*, 126–129.
4. Fu, L.; Lu, H.; Chen, D.; Zhang, R.; Zheng, Y.; Chen, T.; Wei, K.; Liu, X. Field-Dependent Carrier Trapping Induced Kink Effect in AlGa<sub>N</sub>/Ga<sub>N</sub> High Electron Mobility Transistors. *Appl. Phys. Lett.* **2011**, *98*, 173508–173510.
5. Tanaka, K.; Morita, T.; Umeda, H.; Kaneko, S.; Kuroda, M.; Ikoshi, A.; Yamagiwa, H.; Okita, H.; Hikita, M.; Yanagihara, M.; *et al.* Suppression of current collapse by hole injection from drain in a normally-off Ga<sub>N</sub>-based hybrid-drain-embedded gate injection transistor. *Appl. Phys. Lett.* **2015**, *107*, 163502.
6. Sang, L.; Yang, X.; Cheng, J.; Jia, L.; He, Z.; Guo, L.; Hu, A.; Xiang, Y.; Yu, T.; Wang, M.; *et al.* Hysteresis phenomena of the two dimensional electron gas density in lattice-matched InAlN/GaN heterostructures. *Appl. Phys. Lett.* **2015**, *107*, 052102.
7. Harmatha, L.; Stuchlikova, L.; Racko, J.; Marek, J.; Priesol, J.; Benko, P.; Nemeč, M.; Breza, J. Capacitance properties and simulation of the AlGa<sub>N</sub>/Ga<sub>N</sub> Schottky heterostructure. *Appl. Surf. Sci.* **2014**, *312*, 102–106. [[CrossRef](#)]
8. Kamyczek, P.; Placzek-Popko, E.; Zytikiewicz, Z.R.; Zielony, E.; Gumienny, Z. Deep traps in n-type Ga<sub>N</sub> epilayers grown by plasma assisted molecular beam epitaxy. *J. Appl. Phys.* **2014**, *115*, 023102. [[CrossRef](#)]
9. Nguyen, X.S.; Lin, K.; Zhang, Z.; McSkimming, B.; Arehart, A.R.; Speck, J.S.; Ringel, S.A.; Fitzgerald, E.A.; Chua, S. Correlation of a generation-recombination center with a deep level trap in Ga<sub>N</sub>. *J. Appl. Phys. Lett.* **2015**, *106*, 102101. [[CrossRef](#)]
10. Marso, M.; Wolter, M.; Javorka, P.; Kordoš, P.; Lüth, H. Investigation of buffer traps in an AlGa<sub>N</sub>/Ga<sub>N</sub>/Si high electron mobility transistor by backgating current deep level transient spectroscopy. *Appl. Phys. Lett.* **2003**, *82*, 633.
11. Elhaji, A.; Evans-Freeman, J.H.; El-Nahass, M.M.; Kappers, M.J.; Humpries, C.J. Electrical characterization and DLTS analysis of a gold/n-type gallium nitride Schottky diode. *Mater. Sci. Semicond. Process.* **2014**, *17*, 94–99. [[CrossRef](#)]
12. Sasikumar, A.; Arehart, A.R.; Via, G.D.; Heller, E.; Ringel, S.A. Deep trap-induced dynamic on-resistance degradation in Ga<sub>N</sub>-on-Si power MISHEMTs. *Microel. Reliab.* **2016**, *56*, 37–44. [[CrossRef](#)]
13. Lee, J.-G.; Park, B.-R.; Cho, C.-H.; Seo, K.-S.; Cha, H.-Y. Low Turn-On Voltage AlGa<sub>N</sub>/Ga<sub>N</sub>-on-Si Rectifier With Gated Ohmic Anode. *IEEE Electron. Dev. Lett.* **2013**, *34*, 214–216. [[CrossRef](#)]

14. Hu, M.J.; Stoffels, S.; Lenci, S.; Bakeroot, B.; Venegas, R.; Groeseneken, G.; Decoutere, S. Current transient spectroscopy for trapping analysis on Au-free AlGa<sub>N</sub>/Ga<sub>N</sub> Schottky barrier diode. *Appl. Phys. Lett.* **2015**, *106*, 083502.
15. Stoklas, R.; Gregušova, D.; Novák, J.; Vescan, A.; Kordoš, P. Investigation of trapping effects in AlGa<sub>N</sub>/Ga<sub>N</sub>/Si field-effect transistors by frequency dependent capacitance and conductance analysis. *Appl. Phys. Lett.* **2008**, *93*, 124103.
16. Rao, H.; Bosman, G.J. Device reliability study of high gate electric field effects in AlGa<sub>N</sub>/Ga<sub>N</sub> high electron mobility transistors using low frequency noise spectroscopy. *J. Appl. Phys.* **2010**, *108*, 053707.
17. Du, J.; Chen, N.; Jiang, Z.; Bai, Z.; Liu, Y.; Yu, Q. Study on transconductance non-linearity of AlGa<sub>N</sub>/Ga<sub>N</sub> HEMTs considering acceptor-like traps in barrier layer under the gate. *Solid-St. Electron.* **2016**, *115*, 60–64.
18. Miczek, M.; Mizue, C.; Hashizume, T.; Adamowicz, B. Effects of interface states and temperature on the C-VC-V behavior of metal/insulator/AlGa<sub>N</sub>/Ga<sub>N</sub> heterostructure capacitors. *J. Appl. Phys.* **2008**, *103*, 104510. [[CrossRef](#)]
19. Joh, J.; del Alamo, J.A. A Current-Transient Methodology for Trap Analysis for Ga<sub>N</sub> High Electron Mobility Transistors. *IEEE Trans. Electron. Dev.* **2011**, *58*, 132–139. [[CrossRef](#)]
20. Tapajna, M.; Simms, R.J.T.; Pei, Y.; Mishra, U.K.; Kuball, M. Integrated Optical and Electrical Analysis: Identifying Location and Properties of Traps in AlGa<sub>N</sub>/Ga<sub>N</sub> HEMTs During Electrical Stress. *IEEE Electron. Dev. Lett.* **2010**, *31*, 662–664. [[CrossRef](#)]
21. Martin-Horcajo, S.; Wang, A.; Bosca, A.; Romero, M.F.; Tadjer, M.J.; Koehler, A.D.; Anderson, T.J.; Calle, F. Trapping phenomena in AlGa<sub>N</sub> and InAlN barrier HEMTs with different geometries. *Semicond. Sci. Technol.* **2015**, *30*, 035015.
22. Huber, M.; Silvestri, M.; Knuutila, L.; Pozzovivo, G.; Andreev, A.; Kadashchuk, A.; Bonanni, A.; Lundskog, A. Impact of residual carbon impurities and gallium vacancies on trapping effects in AlGa<sub>N</sub>/Ga<sub>N</sub> metal insulator semiconductor high electron mobility transistors. *Appl. Phys. Lett.* **2015**, *107*, 032106.
23. Meneghini, M.; Rossetto, I.; Bisi, D.; Stocco, A.; Chini, A.; Pantellini, A.; Lanzieri, C.; Nanni, A.; Meneghesso, G.; Zanoni, E. Buffer Traps in Fe-Doped AlGa<sub>N</sub>/Ga<sub>N</sub> HEMTs: Investigation of the Physical Properties Based on Pulsed and Transient Measurements. *IEEE Trans. Electron. Dev.* **2014**, *61*, 4070–4077. [[CrossRef](#)]
24. Kang, T.S.; Ren, F.; Gila, B.P.; Pearton, S.J.; Patrick, E.; Cheney, D.J.; Law, M.; Zhang, M.L. Investigation of traps in AlGa<sub>N</sub>/Ga<sub>N</sub> high electron mobility transistors by sub-band gap optical pumping. *J. Vacuum Sci. Technol. B* **2015**, *33*, 061202. [[CrossRef](#)]
25. Donoval, D.; Chvála, A.; Šramatý, R.; Kováč, J.; Morvan, E.; Dua, C.; DiForte-Poisson, M.A.; Kordoš, P. Transport properties and barrier height evaluation in Ni/InAlN/Ga<sub>N</sub> Schottky diodes. *J. Appl. Phys.* **2011**, *109*, 063711. [[CrossRef](#)]



© 2016 by the authors; licensee MDPI, Basel, Switzerland. This article is an open access article distributed under the terms and conditions of the Creative Commons Attribution (CC-BY) license (<http://creativecommons.org/licenses/by/4.0/>).